

Article

Co-Operative Biofilm Interactions between *Aspergillus fumigatus* and *Pseudomonas aeruginosa* through Secreted Galactosaminogalactan Exopolysaccharide

Hanna Ostapska ^{1,2,3}, François Le Mauff ^{1,2,3}, Fabrice N. Gravelat ^{1,2,3}, Brendan D. Snarr ^{1,2,3} ,
Natalie C. Bamford ^{4,5,6}, Jaime C. Van Loon ^{4,5}, Geoffrey McKay ⁷, Dao Nguyen ^{1,7,8}, P. Lynne Howell ^{4,5} ,
and Donald C. Sheppard ^{1,2,3,8,*} 

¹ Department of Microbiology and Immunology, McGill University, Montreal, QC H3A 2B4, Canada; hanna.ostapska@mail.mcgill.ca (H.O.); francois.lemauff@mail.mcgill.ca (F.L.M.); fabrice.gravelat@affiliate.mcgill.ca (F.N.G.); brendan.snarr@mail.mcgill.ca (B.D.S.); dao.nguyen@mcgill.ca (D.N.)

² Infectious Disease in Global Health Program, McGill University Health Centre, Montreal, QC H4A 3J1, Canada

³ McGill Interdisciplinary Initiative in Infection and Immunity, Montreal, QC H3A 1Y2, Canada

⁴ Program in Molecular Medicine, Research Institute, The Hospital for Sick Children, Toronto, ON M5G 0A4, Canada; nbamford001@dundee.ac.uk (N.C.B.); jaime.vanloon@mail.utoronto.ca (J.C.V.L.); howell@sickkids.ca (P.L.H.)

⁵ Department of Biochemistry, University of Toronto, Toronto, ON M5S 1A8, Canada

⁶ Division of Molecular Microbiology, School of Life Sciences, University of Dundee, Dundee DD1 5EH, UK

⁷ Meakins-Christie Laboratories, McGill University Health Centre, Montreal, QC H4A 3J1, Canada; geoffrey.mckay@affiliate.mcgill.ca

⁸ Department of Medicine, McGill University, Montreal, QC H4A 3J1, Canada

* Correspondence: don.sheppard@mcgill.ca



Citation: Ostapska, H.; Le Mauff, F.; Gravelat, F.N.; Snarr, B.D.; Bamford, N.C.; Van Loon, J.C.; McKay, G.; Nguyen, D.; Howell, P.L.; Sheppard, D.C. Co-Operative Biofilm Interactions between *Aspergillus fumigatus* and *Pseudomonas aeruginosa* through Secreted Galactosaminogalactan Exopolysaccharide. *J. Fungi* **2022**, *8*, 336. <https://doi.org/10.3390/jof8040336>

Academic Editor: Clarissa J. Nobile

Received: 18 February 2022

Accepted: 18 March 2022

Published: 24 March 2022

Publisher's Note: MDPI stays neutral with regard to jurisdictional claims in published maps and institutional affiliations.



Copyright: © 2022 by the authors. Licensee MDPI, Basel, Switzerland. This article is an open access article distributed under the terms and conditions of the Creative Commons Attribution (CC BY) license (<https://creativecommons.org/licenses/by/4.0/>).

Abstract: The mold *Aspergillus fumigatus* and bacterium *Pseudomonas aeruginosa* form biofilms in the airways of individuals with cystic fibrosis. Biofilm formation by *A. fumigatus* depends on the self-produced cationic exopolysaccharide galactosaminogalactan (GAG), while *P. aeruginosa* biofilms can contain the cationic exopolysaccharide Pel. GAG and Pel are rendered cationic by deacetylation mediated by either the secreted deacetylase Agd3 (*A. fumigatus*) or the periplasmic deacetylase PelA (*P. aeruginosa*). Given the similarities between these polymers, the potential for biofilm interactions between these organisms were investigated. *P. aeruginosa* were observed to adhere to *A. fumigatus* hyphae in a GAG-dependent manner and to GAG-coated coverslips of *A. fumigatus* biofilms. In biofilm adherence assays, incubation of *P. aeruginosa* with *A. fumigatus* culture supernatants containing de-*N*-acetylated GAG augmented the formation of adherent *P. aeruginosa* biofilms, increasing protection against killing by the antibiotic colistin. Fluorescence microscopy demonstrated incorporation of GAG within *P. aeruginosa* biofilms, suggesting that GAG can serve as an alternate biofilm exopolysaccharide for this bacterium. In contrast, Pel-containing bacterial culture supernatants only augmented the formation of adherent *A. fumigatus* biofilms when antifungal inhibitory molecules were removed. This study demonstrates biofilm interaction via exopolysaccharides as a potential mechanism of co-operation between these organisms in chronic lung disease.

Keywords: biofilm; *Aspergillus fumigatus*; *Pseudomonas aeruginosa*; exopolysaccharide; Pel; galactosaminogalactan (GAG); interaction; co-operation; resistance; cystic fibrosis

1. Introduction

Airway colonization with the mold *Aspergillus fumigatus* and bacterium *Pseudomonas aeruginosa* is common in individuals with chronic lung disease. In individuals with cystic fibrosis, positive respiratory cultures for *A. fumigatus* and *P. aeruginosa* increase in frequency

with age [1–3]. By adulthood, *P. aeruginosa* is the most common bacterium isolated from respiratory cultures, affecting up to 76% of individuals with cystic fibrosis [2]. *A. fumigatus* is the most common filamentous fungus in this population and is isolated in up to 61% of the adult cystic fibrosis population [2]. The co-isolation of *A. fumigatus* and *P. aeruginosa* has been reported in up to 54% of some cohorts [4]. The co-isolation of these two organisms has been associated with poor clinical outcomes, such that individuals that have persistent *A. fumigatus*–*P. aeruginosa* co-infection exhibit a greater decline in lung function than those infected with either organism alone [4]. The frequent recovery of these two organisms from the airways of patients with chronic lung disease suggests that fungal–bacterial interactions may play a role in the pathogenesis of chronic airway disease.

During a co-culture in vitro, *P. aeruginosa* inhibits the germination of *A. fumigatus* conidia [5]. As a result, the majority of studies examining *P. aeruginosa*–*A. fumigatus* interactions have focused on elucidating the mechanisms underlying this inhibition of fungal growth. Several classes of quorum-sensing molecules, including dirhamnolipids, homoserine lactones, quinolones and phenazines, as well as siderophores secreted by *P. aeruginosa*, can inhibit fungal growth, restrict iron acquisition, or induce oxidative stress. The dirhamnolipid surfactant molecules secreted by *P. aeruginosa* for biofilm maintenance can directly inhibit fungal cell wall β -1,3 glucan production, impairing hyphal growth [6,7]. While quinolone-signaling molecules, quinolone 2-heptyl-3-hydroxy-4-quinolone and 2-heptyl-4-quinolone, interfere with conidial germination [8], the mechanism by which homoserine lactone-signaling molecules inhibit fungal growth, and thus biofilm formation is currently unknown [5]. The phenazine 1-hydroxyphenazine, quinolone 2-heptyl-3-hydroxy-4-quinolone, and the extracellular siderophores, pyoverdine and pyochelin, chelate ferric iron, thus restricting fungal access to this important ion and inhibiting growth [9–16]. *P. aeruginosa* can also release an iron-chelating Pf4 bacteriophage that can form an ordered coating on fungal biofilms, thereby limiting hyphal access to iron [17]. At high concentrations, phenazines, including pyocyanin, phenazine-1-carboxylic acid, phenazine-1-carboxamide, as well as phenazine 1-hydroxyphenazine and the siderophore pyochelin, are fungicidal redox-active agents [10–12]. Finally, a spectrum of volatile metabolites released by *P. aeruginosa* has been reported to inhibit *Aspergillus* growth, although the mechanisms by which these molecules inhibit fungal growth are not yet well understood [18].

Although these studies are consistent with the fungal growth inhibition by *P. aeruginosa* that is observed in vitro, these findings contrast with the observation that co-colonization with these organisms is commonly reported in patients with chronic lung disease. Therefore, several studies have focused on the mechanisms by which *P. aeruginosa* and *A. fumigatus* could co-operate. While low levels of pyochelin can sequester iron and impair fungal growth, at higher levels this chelator can transfer iron to the fungal siderophore triacetyl-fusarinine C and stimulate fungal growth [10]. Similarly, sub-inhibitory concentrations of the phenazines pyocyanin, phenazine-1-carboxamide and phenazine-1-carboxylic acid can stimulate fungal growth by facilitating the acquisition of iron by *A. fumigatus* possibly through reducing iron to a more bioavailable ferrous form [11,19,20]. While in a low iron environment, 2-heptyl-3-hydroxy-4-quinolone is inhibitory to fungal growth, in the presence of high iron levels, this quorum-sensing molecule can also enhance fungal metabolism and growth [14]. Further, volatile metabolic by-products containing sulfur groups released by *P. aeruginosa* have been reported to stimulate fungal growth through interactions with the hyphal cell wall [21,22]. Therefore, the outcome of the interactions between *A. fumigatus* and *P. aeruginosa* may depend on airway microenvironmental factors, including the proximity of the organisms, and local concentrations of diffusible molecules.

Biofilm formation is another process where interactions between *P. aeruginosa* and *A. fumigatus* may occur. The biofilms of *A. fumigatus* and *P. aeruginosa* share a common feature in that both organisms can produce cationic partially de-*N*-acetylated exopolysaccharides that are similar in chemical composition and play important roles in biofilm formation [23–27]. Fungal galactosaminogalactan (GAG) is composed of α -1,4-linked D-galactose and partially deacetylated *N*-acetyl-D-galactosamine (GalNAc) and is required for the formation of

A. fumigatus biofilms on most surfaces [23,24,27]. *P. aeruginosa* Pel polysaccharide mediates biofilm formation by some strains of *P. aeruginosa* [26] and is composed of GalNAc and *N*-acetyl-D-glucosamine, one or both of which are de-*N*-acetylated [28] resulting in a 50% acetylated polymer [29]. Deacetylation plays an important role in the function of both exopolysaccharides by rendering the polymers cationic and adhesive to anionic surfaces [23,25]. The presence of Pel has been demonstrated in *P. aeruginosa* biofilm aggregates in the sputum of patients with cystic fibrosis, suggesting it may play an important role in biofilm formation in vivo [29].

GAG and Pel biosynthesis share several similarities [30]. GAG synthesis begins with the production of the nucleotide monosaccharides uridine diphosphate (UDP)-galactopyranose and UDP-GalNAc by the epimerase Uge3 [23]. These sugars are then polymerized and exported by the putative transmembrane glycosyl transferase Gtb3 [31] where deacetylation of GAG then extracellularly occurs by the secreted deacetylase Agd3 [24]. An Agd3-deficient $\Delta agd3$ mutant produces fully *N*-acetylated GAG that cannot adhere to hyphae or support biofilm formation [24]. These defects can be restored with the addition of extracellular recombinant Agd3 (rAgd3) [32]. Pel synthesis is similar to GAG in that it is mediated by an inner-membrane multi-protein complex that includes the glycosyl transferase PelF [31,33]. However, Pel is deacetylated within the periplasm through the action of the deacetylase domain of the PelA protein, and is exported as the mature polymer, a process that requires both the membrane-anchored funnel protein PelC and the porin PelB [31,34]. The *P. aeruginosa* PA14 strain is a clinical strain originally isolated from a burn wound [35] that forms Pel-dominant biofilms, as this strain is genetically capable of producing only Pel and not Psl. PA14 is, therefore, the most commonly used isolate for studying Pel-dependent phenotypes [26,36,37]. A *P. aeruginosa* PA14 $\Delta pelA$ mutant deficient in PelA expression fails to produce secreted Pel; consequently, it lacks the capacity to form biofilms [25]. In contrast, while the clinical isolate and reference strain *P. aeruginosa* PAO1 [38] contains both the Pel and Psl operons, this strain forms Psl-dominant biofilms, and a mutation in *pelA* does not compromise biofilm development [36,39,40]. The similarities in the synthesis and composition of secreted GAG and Pel matrix exopolysaccharides suggests the hypothesis that GAG and/or Pel may mediate co-operative biofilm formation between *A. fumigatus* and *P. aeruginosa*.

Herein, we identified a co-operative interaction between *A. fumigatus* and *P. aeruginosa* at the level of biofilm formation. Confocal and scanning electron microscopy imaging of *P. aeruginosa* with *A. fumigatus* mutant strains during biofilm formation revealed that secreted GAG can mediate *P. aeruginosa* adherence to *A. fumigatus* biofilms. Crystal violet staining demonstrated that wild-type *A. fumigatus* culture supernatants containing secreted GAG can augment the formation of adherent *P. aeruginosa* biofilms. This augmentation is GAG-dependent as culture supernatants from the GAG-deficient $\Delta uge3$ mutant fungal strain failed to augment adherent bacterial biofilm formation. Culture supernatants containing fully *N*-acetylated GAG from the $\Delta agd3$ mutant fungal strain augmented *P. aeruginosa* biofilms only when combined with the rAgd3 deacetylase enzyme, suggesting that de-*N*-acetylated GAG is required for this phenotype. Fluorescence confocal microscopy imaging revealed that de-*N*-acetylated GAG incorporates directly into *P. aeruginosa* biofilms, suggesting that GAG may play a structural role in these bacterial biofilms. A functional role for the GAG augmentation of *P. aeruginosa* biofilms was supported by the observation that GAG augmentation protected bacteria against killing by the antibiotic colistin. Although Pel-containing bacterial culture supernatants could augment fungal biofilm biomass adherence, this effect was only detectable when culture supernatants were dialyzed to remove substances that inhibit fungal growth. Collectively, these findings provide a potential mechanism for co-operation between these two organisms within the airways of patients with chronic airway disease.

2. Materials and Methods

2.1. Fungal and Bacterial Strains and Growth Conditions

A. fumigatus and *P. aeruginosa* strains used in this study are detailed in Table S1. *A. fumigatus* strains were grown on yeast extract-peptone-dextrose (BD Biosciences Difco™, Franklin Lakes, NJ, USA) agar (BD Biosciences Difco™ Bacteriological, Franklin Lakes, NJ, USA) plates at 37 °C, from −80 °C stocks. Conidia were harvested following 6 days of growth with phosphate-buffered saline (PBS, HyClone, Logan, UT, USA) containing 0.1% Tween 80 (Fisher Scientific, Pittsburgh, PA, USA) (PBS-T), washed and resuspended in PBS-T. *A. fumigatus* was grown in Luria-Bertani broth (LB, BD™ Difco™ Miller LB, Franklin Lakes, NJ, USA) or phenol-free RPMI 1640 (Phenol Red-, HEPES-, L-Glutamine-free, Wisent, St-Bruno, QC, Canada) as indicated at 37 °C and in 5% CO₂. *P. aeruginosa* strains were grown on LB agar plates overnight at 37 °C, from −80 °C stocks. *P. aeruginosa* strains were cultured overnight at 37 °C in LB alone or LB supplemented with 250 µg/mL carbenicillin (Sigma, Burlington, VT, USA) and/or with or without 0.5% L-arabinose (BioShop, Burlington, ON, Canada) as indicated.

2.2. Construction of Red Fluorescent Protein (mCherry)-Producing and Green Fluorescent Protein (GFP)-Producing *P. aeruginosa* Strains

To image interactions with *P. aeruginosa*, bacterial strains were transformed by electroporation as previously described [41], with the pMKB1::mCherry plasmid containing the gene encoding the monomeric second-generation red fluorescent protein (RFP) mCherry or by chemical transformation as previously described [42], with the pMKB1::gfp plasmid containing the gene encoding the green fluorescent protein (GFP). Transformants were selected by resistance to carbenicillin (250 µg/mL).

2.3. Construction of the GFP-Producing *A. fumigatus* Δ uge3 Mutant Strain

To image interactions with the *A. fumigatus* Δ uge3 mutant strain, *A. fumigatus* Δ uge3 spheroplasts [43] were transformed with a linearized pGFP-ble plasmid encoding GFP and phleomycin resistance. Transformants were screened by resistance to phleomycin (150 µg/mL) [43] and GFP production was confirmed with microscopy.

2.4. Galactomannan Quantification in Fungal–Bacterial Interactions by Immunoassay

For conidia co-culture experiments, flasks were inoculated with 1×10^6 *A. fumigatus* conidia/mL in 100 mL LB and 5.5×10^7 *P. aeruginosa* CFU/mL in LB then incubated at 37 °C. For hyphal experiments, fungal cultures were grown for 13 h and then inoculated with bacteria. Culture supernatants were sampled at 18 and 24 h, and galactomannan content of culture supernatants was determined by using the Platelia™ Aspergillus immunoassay kit (Bio-Rad, Hercules, CA, USA), according to the manufacturer's instructions. Relative fungal growth was determined by comparing the resulting optical density values to an internal standard curve generated using serial dilutions of a pool of lung homogenates from five highly immunosuppressed mice infected with *A. fumigatus* strain Af293, as carried out previously [44–49].

2.5. Scanning Electron Microscopy

For studies of direct fungal–bacterial interactions, samples of co-cultured *A. fumigatus* hyphae with *P. aeruginosa* were prepared for scanning electron microscopy using a modification of our previously described dehydration and coating procedure [23]. Hyphae were grown on glass coverslips for 24 h in RPMI 1640. 9.0×10^7 bacterial CFU/mL were co-incubated with hyphae for 0.5 h. Hyphae were washed with PBS and fixed with 2.5% glutaraldehyde (Electron Microscopy Sciences, Hatfield, PA, USA) in 0.1 M cacodylate buffer (BioShop, Burlington, ON, Canada) at room temperature, sequentially dehydrated in ethanol (Commercial alcohols, Toronto, ON, Canada) and then critical-point dried in CO₂. Coverslips were mounted onto studs and sputter coated with Au-Pd. Hyphae were

imaged with field-emission scanning electron microscopy (S-4700 FESEM, Hitachi, Tokyo, Japan) at 10,000 \times and 5000 \times .

2.6. Confocal Microscopy

For studies of direct fungal–bacterial interactions, cultures of mCherry-producing bacteria supplemented with 250 $\mu\text{g}/\text{mL}$ carbenicillin, with or without 0.5% L-arabinose, were co-incubated with GFP-producing hyphae grown in LB as described above; hyphae were washed with PBS and fixed with 1% paraformaldehyde (Electron Microscopy Sciences, Hatfield, PA, USA) for 1 h at 4 $^{\circ}\text{C}$. Hyphae were washed with PBS and mounted on SlowFade™ (Thermo Fisher Scientific, Waltham, MA, USA), then imaged by confocal microscopy (Zeiss LSM700, Zeiss, Oberkochen, Germany) with 488 and 555 nm lasers at 630 \times .

For visualization of GAG in bacterial biofilms, co-cultures of *P. aeruginosa* with *A. fumigatus* culture supernatants were grown and stained in a modified version of the previously described chamber coverglass system [50]. An amount of 200 μL of 9.0×10^7 *P. aeruginosa* CFU/mL in LB were grown in 8-well borosilicate glass, non-removable well chambers (Nunc™ Lab-Tec™ II Chambered System, Thermo Fisher, Waltham, MA, USA) with a combination of 640 μL *N*-acetylated-GAG-containing *A. fumigatus* culture supernatants and 165 nM recombinant Agd3 (rAgd3) [32] or LB alone for 24 h. Culture supernatants were then removed and biofilms were stained with a 1:800 dilution of anti-GalNAc antibody (a generous gift from Jean-Paul Latgé, Institute Pasteur, Paris, France) in PBS with 0.2% goat serum (Gibco, Waltham, MA, USA) overnight at room temperature. Biofilms were washed with PBS and further stained with a 1:200 dilution of a secondary Alexa Flour-488 conjugated antibody (Invitrogen™, Waltham, MA, USA) overnight at room temperature, then counter stained with a 1:250 dilution of DRAQ5™ (eBioscience, Waltham, MA, USA) overnight at 4 $^{\circ}\text{C}$. Biofilms were imaged by confocal microscopy as above. For visualization of GAG with the recombinant carbohydrate-binding module Agd3 (Agd3¹⁴¹⁻³⁶⁴), *P. aeruginosa* biofilms were stained with our previously described GAG binding assay [32]. Biofilms of mCherry-producing *P. aeruginosa* were grown with 250 $\mu\text{g}/\text{mL}$ carbenicillin (Sigma, Burlington, VT, USA). Biofilms were stained with 10 μM Alexa Flour-568 labeled Agd3¹⁴¹⁻³⁶⁴ [32] for 2 h at 4 $^{\circ}\text{C}$, washed twice with PBS and fixed with 4% paraformaldehyde. Biofilms were imaged by confocal microscopy as above. Mean fluorescent intensity was determined with ImageJ (version 1.52a) software (National Institutes of Health, Bethesda, MD, USA).

2.7. Culture Supernatant Collection

Fungal culture supernatants were prepared in flasks inoculated with 1×10^6 *A. fumigatus* conidia/mL in 100 mL LB and incubated at 37 $^{\circ}\text{C}$ [23]. After 26 h, culture supernatants were filtered through either a 0.22 μm nylon membrane (Steritop™, Waltham, MA, USA) or Miracloth (Millipore Sigma, Burlington, ON, Canada). Culture supernatants were either lyophilized (Labconco, Kansas City, MO, USA) or stored at -20 $^{\circ}\text{C}$.

Bacterial culture supernatants were prepared in flat-bottom, non-tissue, culture-treated, 24-well plates (Falcon, Burlington, VT, USA) inoculated with 2 mL of 9.0×10^7 *P. aeruginosa* CFU/mL in LB per well with or without 0.5% L-arabinose (BioShop, Burlington, ON, Canada) and statically incubated at 37 $^{\circ}\text{C}$. 48 h old culture supernatants were aspirated, separated from bacteria by centrifugation (Sorvall Legend RT+, Thermo Scientific, Waltham, MA, USA) at 2643 \times *g* for 30 min, and residual planktonic bacteria were heat-killed for 1 h at 60 $^{\circ}\text{C}$ [6]. Culture supernatants were dialyzed through 3.5 kDa molecular weight cut-off cellulose membrane (Fisherbrand, Pittsburgh, PA, USA or Spectrum Labs, Waltham, MA, USA) in 2 passes of deionized water, 1 pass of deionized water with 0.2% sodium azide (BioShop, Burlington, ON, Canada), 3 additional passes of deionized water, and 3 passes of 0.1% PBS. Culture supernatants were then either lyophilized or stored at 4 $^{\circ}\text{C}$.

2.8. Crystal Violet Biomass Adherence Assay

For studies of bacterial biofilm adherence, adherent biofilm biomass was quantified using a modification of the previously described assay [51]. Bacterial biofilms were grown in flat-bottom, non-tissue, culture-treated, 96-well plates (Falcon, Burlington, VT, USA) that were inoculated with 100 μL of 9.0×10^7 *P. aeruginosa* CFU/mL in LB and diluted 1:2 with a combination of 50 μL LB and 50 μL of *A. fumigatus* or *P. aeruginosa* culture supernatants or LB alone. For biofilm deacetylation studies, 130 nM rAgd3 was added to plates that were prepared as described above. Plates were incubated for 22 h at 37 °C and then washed with 300 μL deionized water and stained with 200 μL 0.1% crystal violet (BioShop, Burlington, ON, Canada) for 10 min. Crystal violet was solubilized with 200 μL ethanol (Commercial alcohols, Toronto, ON, Canada) for 10 min, and the absorbance of 150 μL of the solution was measured at 600 nm (Tecan Infinite M200PRO, Tecan, Mannedorf, Switzerland).

For studies of fungal biofilm adherence, adherent biofilm biomass was quantified using a modification of our previously described crystal violet assay [42]. Fungal biofilms were grown in round-bottom, non-tissue, culture-treated, 96-well plates (Falcon, Burlington, VT, USA) that were inoculated with 1×10^6 *A. fumigatus* conidia/mL in 50 μL LB and 50 μL of *P. aeruginosa* or *A. fumigatus* culture supernatants or LB alone and incubated for 20 h at 37 °C in 5% CO₂. Plates were washed with 100 μL deionized water and stained with 100 μL 0.1% crystal violet for 10 min. Crystal violet was solubilized with 100 μL ethanol for 10 min, and the absorbance of the resulting solution was measured as above.

2.9. Antibiotic Susceptibility Assay

For antimicrobial challenge of augmented adhered bacterial biomass, bacterial biofilms were grown in the presence of fungal culture supernatants as described above. Antimicrobial treatment was performed using a modified version of our previously described antibiotic susceptibility assay [51]. Briefly, 22 h old biofilms were washed with PBS and treated with 250 μL of 1.17 $\mu\text{g}/\text{mL}$ colistin sulfate salt (Sigma, Burlington, VT, USA) in PBS for 5 h at 37 °C in 5% CO₂. Bacterial viability was measured using a modification of a previously described XTT tetrazolium salt (2,6-bis-(2-methoxy-4-nitro-5-sulfophenyl)-2H-tetrazolium-5-carboxanilide) metabolic assay [52]. Briefly, 50 μL XTT tetrazolium salt solution (100 $\mu\text{g}/\text{mL}$ XTT tetrazolium salt (BioShop, Burlington, ON, Canada) and 25 μM menadione (Sigma, Burlington, VT, USA) was added to wells and plates were incubated at 37 °C in the dark for 2 h. The absorbance of 180 μL of the solution was measured at 450 nm (Tecan Infinite M200PRO, Tecan, Mannedorf, Switzerland).

2.10. GAG Quantification by Enzyme-Linked Lectin Assay (ELLA)

GAG was quantified in fungal culture supernatants using a modified version of our previously described ELLA [32]. *N*-acetylated or de-*N*-acetylated GAG-containing *A. fumigatus* culture supernatants were serially diluted in TRIS-buffered saline (TBS, Alfa Aesar, Haverhill, MA, USA) in 96-well Immulon 4HBX plates (Thermo Scientific, Waltham, MA, USA). *N*-acetylated GAG-containing culture supernatants were de-*N*-acetylated with 130 nM rAgd3 for 1 h at room temperature. Plates were washed 3 times with TBS with 0.05% Tween 20 (T20, BioShop, Burlington, ON, Canada), stained with lectin solution (30 nM biotinylated soybean agglutinin (Vector Labs, Burlingame, CA, USA) and a 1:700 dilution of avidin conjugated to horseradish peroxidase (Invitrogen)) at room temperature for 1 h. Plates were washed 3 times with TBS-T20 and developed with 3,3',5,5'-tetramethylbenzidine (TMB) substrate ultrasensitive solution (Millipore, Burlington, VT, USA) and 1 M H₂SO₄ (BioShop, Burlington, ON, Canada) stop solution. Absorbance was measured at 450 nm (Tecan Infinite M200PRO, Tecan, Mannedorf, Switzerland).

2.11. Statistical Analysis

Data are presented and statistical significance is calculated as indicated. All graphs were generated, and statistical analyses were performed in GraphPad Prism (version 9.0.0) software (GraphPad, San Diego, CA, USA). Significant differences between values were

compared by one-way analysis of variance (ANOVA) with Tukey's multiple-comparison test, paired *t* test and unpaired *t* test as noted in the figure legends.

3. Results

3.1. *A. fumigatus* Hyphae Are More Resistant Than Conidia to the Inhibitory Effects of *P. aeruginosa*

To determine the effect of *P. aeruginosa* on the growth of different *A. fumigatus* morphologies, bacteria were co-cultured with either *A. fumigatus* conidia or hyphae, and relative fungal growth was monitored by quantifying the relative levels of a secreted fungal exopolysaccharide, galactomannan, over time by immunoassay. Galactomannan is constitutively produced by *A. fumigatus* hyphae and has been used as a surrogate to quantify the growth kinetics of hyphae, which correlate to fungal burden in vivo [42,44–49,53–55]. Even after 24 h of growth, only low levels of galactomannan were detected in co-cultures of *P. aeruginosa* with *A. fumigatus* conidia, consistent with prior reports that *P. aeruginosa* strongly inhibits *A. fumigatus* conidial germination (Figure 1a) [5]. In contrast, when *P. aeruginosa* were added to pre-grown *A. fumigatus* hyphae (13 h), no significant decrease in galactomannan production was observed between hyphae cultured with and without bacteria at up to 24 h after bacterial inoculation (Figure 1b). These results suggest that *A. fumigatus* hyphae are more resistant than conidia to the inhibitory effects of *P. aeruginosa*.

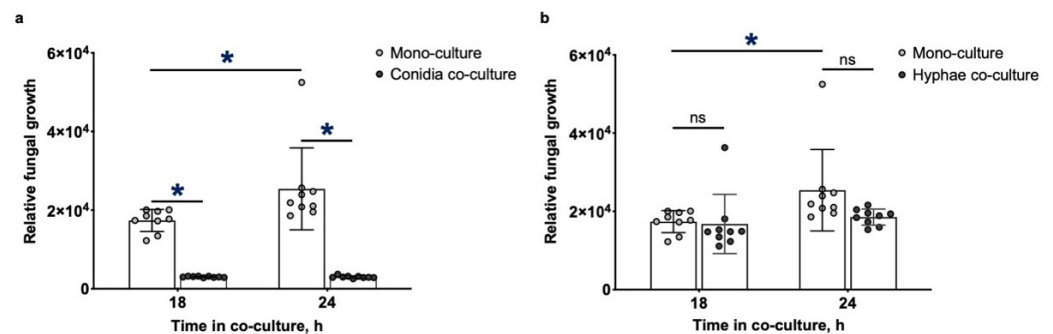


Figure 1. *A. fumigatus* hyphae are more resistant than conidia to the growth inhibitory effects of *P. aeruginosa* during co-culture. (a) Growth of *A. fumigatus* conidia in co-culture with *P. aeruginosa* and (b) growth of *A. fumigatus* pre-grown hyphae in co-culture with *P. aeruginosa* was monitored by quantifying relative galactomannan (GM) over time using a GM enzyme immunoassay (EIA). Bars represent the means \pm standard deviations of 3 independent experiments. A significant increase in growth is indicated by * ($p < 0.05$) and no significant difference in growth is indicated by ns as determined by unpaired *t* test.

3.2. GAG but Not Pel Is Required for Adherence of *P. aeruginosa* to *A. fumigatus* Biofilms

The ability of *A. fumigatus* hyphae to persist in the presence of *P. aeruginosa* suggests that bacteria could interact with fungal biofilms produced by *A. fumigatus* hyphae within co-infected lungs. To begin to probe the direct interactions between fungal biofilms and bacteria, confocal microscopy was used to image biofilms produced by green fluorescent protein (GFP)-producing wild-type *A. fumigatus* co-cultured with the red-fluorescent protein (mCherry)-producing wild-type *P. aeruginosa* strain PA14. Confocal imaging of these co-cultures after washing revealed the presence of abundant *P. aeruginosa* adherent to fungal biofilms, with notable clustering of bacterial cells surrounding *A. fumigatus* hyphae (Figure 2a). Pel-deficient $\Delta pelA$ *P. aeruginosa* exhibited similar levels of adherence to wild-type *A. fumigatus* biofilms as the wild-type bacteria (Figure 2a,b). However, both wild-type *P. aeruginosa* and Pel-deficient $\Delta pelA$ *P. aeruginosa* were found to poorly adhere to GAG-deficient $\Delta uge3$ *A. fumigatus* hyphae (Figure 2c,d). Taken together, these findings suggest that GAG, and not Pel, is required for the adhesion of *P. aeruginosa* to fungal hyphae within biofilms. To test if the inability of Pel to compensate for the loss of GAG was a consequence of insufficient levels of Pel production by *P. aeruginosa* PA14, the ability of a *P. aeruginosa* PAO1 Pel-overexpressing $\Delta wspF\Delta psIP_{BAD}pel$ mutant strain (which also lacks the ability

to produce the Psl polysaccharide) to adhere to GAG-deficient hyphae was tested. As with wild-type bacteria, the Pel-overexpressing $\Delta wspF\Delta psIP_{BAD}pel$ strain adhered well to wild-type fungal biofilms (Figure 2e). However, Pel-overproduction did not augment bacterial adherence to GAG-deficient $\Delta uge3$ hyphae (Figure 2f). Collectively, these findings suggest that GAG, but not Pel, mediates *P. aeruginosa* adherence to *A. fumigatus* biofilms.

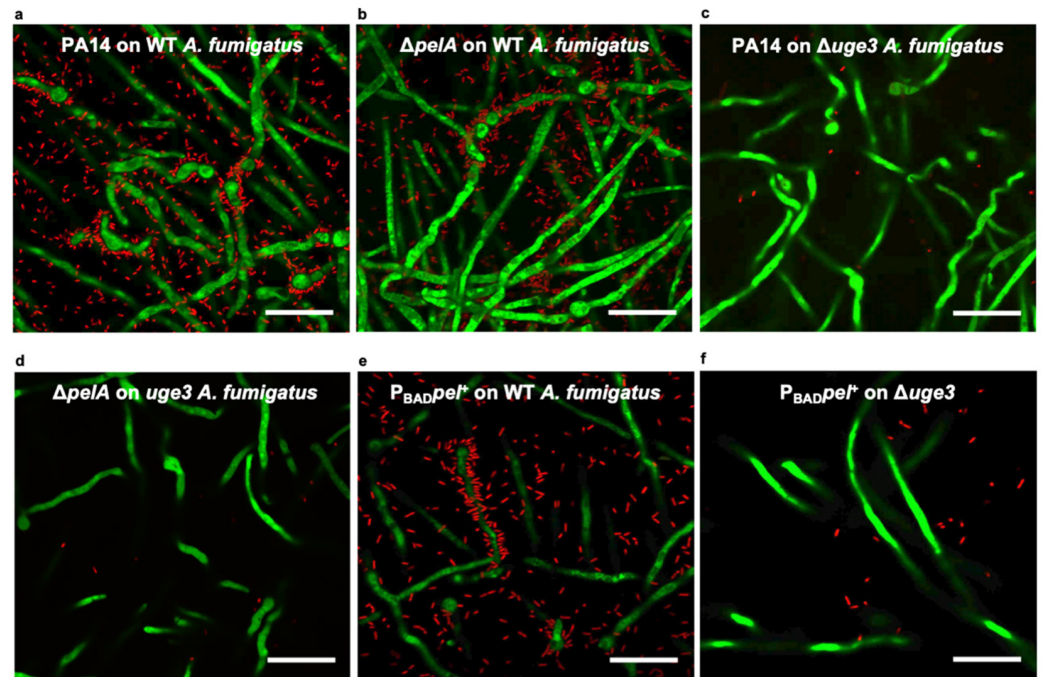


Figure 2. GAG but not Pel is required for the adherence of *P. aeruginosa* to *A. fumigatus*. Confocal microscopy images of green fluorescent protein (GFP)-producing *A. fumigatus* co-cultured with mCherry-producing *P. aeruginosa*. (a) Wild-type *P. aeruginosa* (PA14) adherent to hyphae of wild-type (WT) *A. fumigatus*. (b) Pel-deficient *P. aeruginosa* ($\Delta pelA$) adherent to hyphae of WT *A. fumigatus*. (c) Wild-type *P. aeruginosa* (PA14) not adherent to hyphae of GAG-deficient *A. fumigatus* ($\Delta uge3$). (d) Pel-deficient *P. aeruginosa* ($\Delta pelA$) not adherent to hyphae of GAG-deficient *A. fumigatus* ($\Delta uge3$). (e) Pel-overexpressing $\Delta wspF\Delta psIP_{BAD}pel$ *P. aeruginosa* ($P_{BAD}pel^+$) adherent to hyphae of WT *A. fumigatus*. (f) Pel-overexpressing $\Delta wspF\Delta psIP_{BAD}pel$ *P. aeruginosa* ($P_{BAD}pel^+$) not adherent to hyphae of GAG-deficient *A. fumigatus*. Representative images of at least 2 independent experiments. Imaged at $630\times$ (scale bar, 20 μm).

To confirm these findings and better define the localization of *P. aeruginosa* within fungal biofilms, the scanning electron microscopy of fungal biofilms co-cultured with *P. aeruginosa* was performed. The scanning electron microscopy examination of the wild-type *P. aeruginosa* PA14 strain co-cultured with wild-type *A. fumigatus* biofilms confirmed the presence of bacteria directly adherent to fungal hyphae within fungal biofilms (Figure 3a). As was observed by confocal microscopy, the adherence of *P. aeruginosa* to *A. fumigatus* hyphae appeared to be dependent on the production of fungal GAG and not Pel, as wild-type *P. aeruginosa* and Pel-deficient $\Delta pelA$ *P. aeruginosa* were rarely observed bound to GAG-deficient $\Delta uge3$ hyphae (Figure 3b,c), whereas wild-type and Pel-deficient *P. aeruginosa* were both observed to bind in large numbers to wild-type *A. fumigatus* hyphae (Figure 3a,d). These data are consistent with the hypothesis that fungal GAG is necessary for the adherence of *P. aeruginosa* to hyphae within fungal biofilms.

In addition to the population of hyphal-bound bacteria, wild-type and Pel-deficient $\Delta pelA$ *P. aeruginosa* organisms were also observed to bind to coverslips in the interstitial space between wild-type *A. fumigatus* hyphae (Figure 3a,d). In contrast, few wild-type *P. aeruginosa* were observed on the coverslips of the biofilm-deficient $\Delta uge3$ hyphae (Figure 3e). These findings suggest that, in addition to binding to *A. fumigatus* hyphae,

P. aeruginosa may adhere to secreted biofilm components that are adherent to the surface of coverslips.

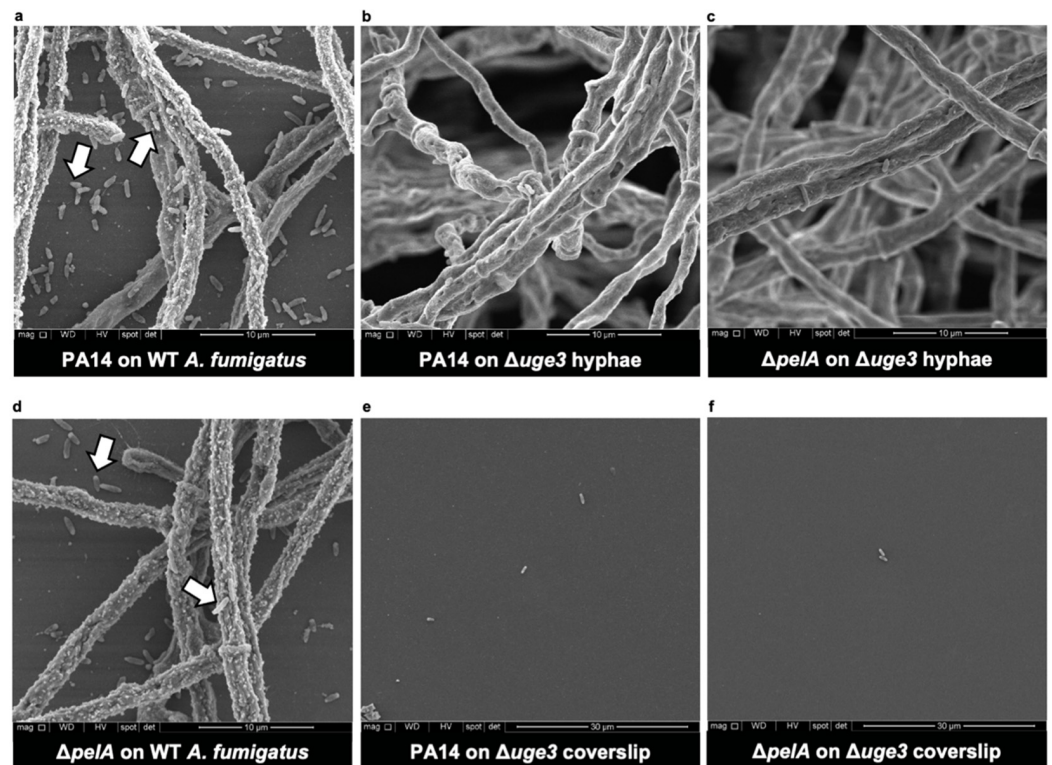


Figure 3. GAG mediates the adherence of *P. aeruginosa* to *A. fumigatus* hyphae. Scanning electron microscopy images of co-cultures of wild-type *P. aeruginosa* (PA14) with (a) adherent wild-type (WT) *A. fumigatus* hyphae on coverslips or (b) non-adherent GAG-deficient *A. fumigatus* hyphae ($\Delta uge3$). Co-cultures of Pel-deficient *P. aeruginosa* ($\Delta pelA$) with (c) non-adherent GAG-deficient *A. fumigatus* hyphae ($\Delta uge3$) or with (d) adherent wild-type *A. fumigatus* hyphae (WT) on coverslips. (e) Coverslip of (b) and (f) coverslip of (c). Representative images of 2 independent experiments. (a–d) Imaged at 10,000 \times . (e,f) Note a lower magnification at 5000 \times . White arrows indicate adherent bacteria to hyphae and coverslips in the interstitial spaces between hyphae.

3.3. Bacterial-Adherent Biofilm Formation Is Augmented by Secreted Fungal Products

Given the observation that the adherence of *P. aeruginosa* to an abiotic surface was enhanced with products secreted into the biofilm matrix by *A. fumigatus* hyphae, we hypothesized that products secreted by *A. fumigatus* could augment the formation of adherent *P. aeruginosa* biofilms. To test this hypothesis and quantify this phenomenon, culture supernatants were collected from *A. fumigatus* and co-cultured with *P. aeruginosa* in static culture in round bottom non-tissue culture-treated 96-well plates (biofilm-forming conditions). Adherent biofilm formation was quantified with crystal violet staining. *P. aeruginosa* co-cultured with *A. fumigatus* culture supernatants exhibited increased adherent biofilm formation compared with bacteria cultured in media alone (Figure 4a). Given that *P. aeruginosa* adhered poorly to coverslips in the presence of the GAG-deficient *A. fumigatus* $\Delta uge3$ mutant (Figure 3e), we hypothesized that secreted GAG was the biofilm matrix product that was responsible for the fungal-mediated augmentation of adherent *P. aeruginosa* biofilm formation. Consistent with this hypothesis, culture supernatants from the GAG-deficient $\Delta uge3$ mutant failed to increase *P. aeruginosa*-adherent biofilm formation (Figure 4a). The presence of GAG in wild-type culture supernatants was confirmed by a GAG-enzyme-linked lectin assay (Supplementary Figure S1). Culture supernatants from wild-type *A. fumigatus*, but not the GAG-deficient $\Delta uge3$ mutant, also resulted in increased the adherent biofilm formation of the Pel-deficient $\Delta pelA$ *P. aeruginosa* mutant, suggesting that Pel

polysaccharide is not required for the GAG-mediated augmentation of adherent bacterial biofilm formation (Figure 4b).

The inability of culture supernatants from the GAG-deficient *A. fumigatus* $\Delta uge3$ mutant to augment *P. aeruginosa* adherent biofilm formation suggests that secreted GAG is responsible for the observed fungal-mediated effects on *P. aeruginosa* biofilm. This observation also suggests that the fungal-mediated augmentation of wild-type *P. aeruginosa* adherence is not a consequence of increased deacetylation of Pel polysaccharide by the secreted fungal deacetylase Agd3, as the $\Delta uge3$ mutant secretes active Agd3 (112). As purified GAG is insoluble, to confirm that Agd3 alone cannot directly increase adherent bacterial biofilm formation, wild-type *P. aeruginosa* and the Pel deacetylase-deficient $\Delta pelA$ mutant were grown in the presence of recombinant Agd3 (rAgd3). As predicted, in comparison to bovine serum albumin protein, rAgd3 treatment did not increase adherent biofilm formation by either bacterial strain (Supplementary Figure S2). Collectively, these data suggest that the fungal-mediated augmentation of *P. aeruginosa* adherent biofilm formation is mediated via GAG polysaccharide rather than the activity of the fungal deacetylase on Pel polysaccharide.

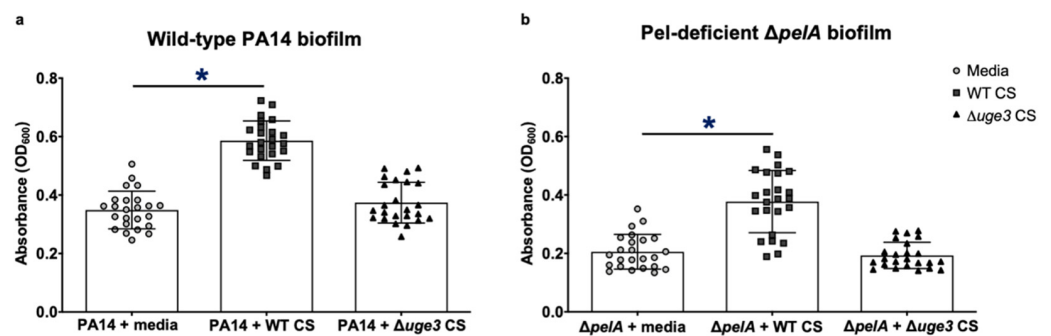


Figure 4. *A. fumigatus*-secreted products increase the formation of *P. aeruginosa*-adherent biofilms. Crystal violet quantification of adherent biofilm biomass by (a) wild-type *P. aeruginosa* (PA14) and (b) Pel-deficient *P. aeruginosa* ($\Delta pelA$) grown in the presence of media control, wild-type *A. fumigatus* culture supernatants (WT CS), or GAG-deficient *A. fumigatus* culture supernatants ($\Delta uge3$ CS). Bars represent the means \pm standard deviations of the destain solution measured at 600 nm of 3 independent experiments. A significant increase in absorbance is indicated by * ($p < 0.0001$) relative to all bars as determined by one-way ANOVA with Tukey's multiple-comparison test.

To determine if the deacetylation of GAG is required for augmentation of bacterial adherent biofilm formation, the Pel-deficient $\Delta pelA$ mutant was co-cultured with culture supernatants from the Agd3-deficient $\Delta agd3$ *A. fumigatus* mutant, which produces only fully *N*-acetylated GAG [24]. In contrast to de-*N*-acetylated GAG-containing wild-type *A. fumigatus* culture supernatants, *A. fumigatus* culture supernatants containing fully *N*-acetylated-GAG failed to augment *P. aeruginosa*-adherent biofilm formation (Figure 5). Together, these results suggest that de-*N*-acetylated, rather than *N*-acetylated GAG, is the secreted product in wild-type *A. fumigatus* culture supernatants that augments adherence of the bacterial biofilms.

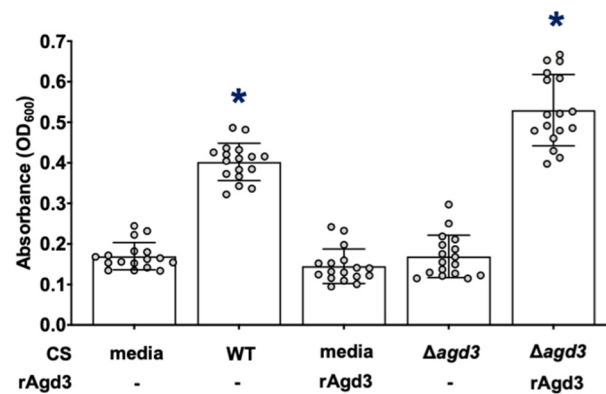


Figure 5. De-*N*-acetylated GAG is required to increase adherent biofilm formation by Pel-deficient *P. aeruginosa*. Adherent biofilm formation by Pel-deficient *P. aeruginosa* ($\Delta pelA$) grown in the presence of de-*N*-acetylated GAG from WT de-*N*-acetylated GAG-containing CS (WT CS), 130 nM recombinant Agd3 deacetylase enzyme (rAgd3) or *N*-acetylated GAG from *N*-acetylated-GAG-containing culture supernatants ($\Delta agd3$ CS), or de-*N*-acetylated GAG from a combination of *N*-acetylated-GAG-containing culture supernatants and 130 nM rAgd3 ($\Delta agd3$ CS + rAgd3) was quantified with crystal violet staining. Bars represent the means \pm standard deviations of 3 independent experiments. A significant increase in absorbance is indicated by * ($p < 0.0001$) relative to all bars as determined by one-way ANOVA with Tukey's multiple-comparison test.

3.4. Secreted GAG Integrates into the Architecture of *P. aeruginosa* Biofilms

To determine if de-*N*-acetylated GAG augments the adherence of bacterial biofilm biomass through direct incorporation into the biofilm matrix, adherent wild-type *P. aeruginosa* biofilms treated with the combination of rAgd3 and *N*-acetylated-GAG-containing culture supernatants were stained with a monoclonal anti-GAG antibody [27]. Immunofluorescence microscopy demonstrated that this antibody stained both wild-type and GAG-treated *P. aeruginosa*-adherent biofilms (Figure 6a), suggesting that this antibody likely detects α -1,4-linked GalNAc regions that are shared by both polymers. However, GAG-treated *P. aeruginosa*-adherent biofilms exhibited significantly higher staining than wild-type *P. aeruginosa* biofilms (mean fluorescence intensity of 39.3 vs. 18.1, respectively), suggesting that de-*N*-acetylated GAG may incorporate into the *P. aeruginosa* biofilm architecture (Figure 6a).

To confirm that the observed increase in fluorescence intensity detected with anti-GalNAc staining was a consequence of incorporating GAG into the biofilm matrix, rather than from the upregulation of Pel production, we exploited the specificity of Agd3 binding to GalN/GalNAc regions of the GAG polymer [32]. Native and GAG-treated *P. aeruginosa* biofilms were incubated with a fluorophore-labeled recombinant carbohydrate binding module of Agd3 (Agd3¹⁴¹⁻³⁶⁴) and then imaged with confocal microscopy to detect GAG. Consistent with our GalNAc antibody staining results, fluorescence microscopy revealed Agd3¹⁴¹⁻³⁶⁴ binding to GAG-treated, GFP-producing, wild-type *P. aeruginosa* biofilms (mean fluorescence intensity of 48.0) (Figure 6b). In contrast, wild-type *P. aeruginosa* biofilms and those grown in the presence of fully *N*-acetylated-GAG-containing culture supernatants did not bind Agd3¹⁴¹⁻³⁶⁴, confirming the GAG specificity of Agd3¹⁴¹⁻³⁶⁴ (mean fluorescence intensity of 4.8 and 10.5, respectively) (Figure 6b). Collectively, these results suggest that the fungal augmentation of bacterial-adherent biofilms is a result of the incorporation of the GAG polymer as a structural element into the biofilm architecture, rather than of GAG-mediated induction of Pel production.

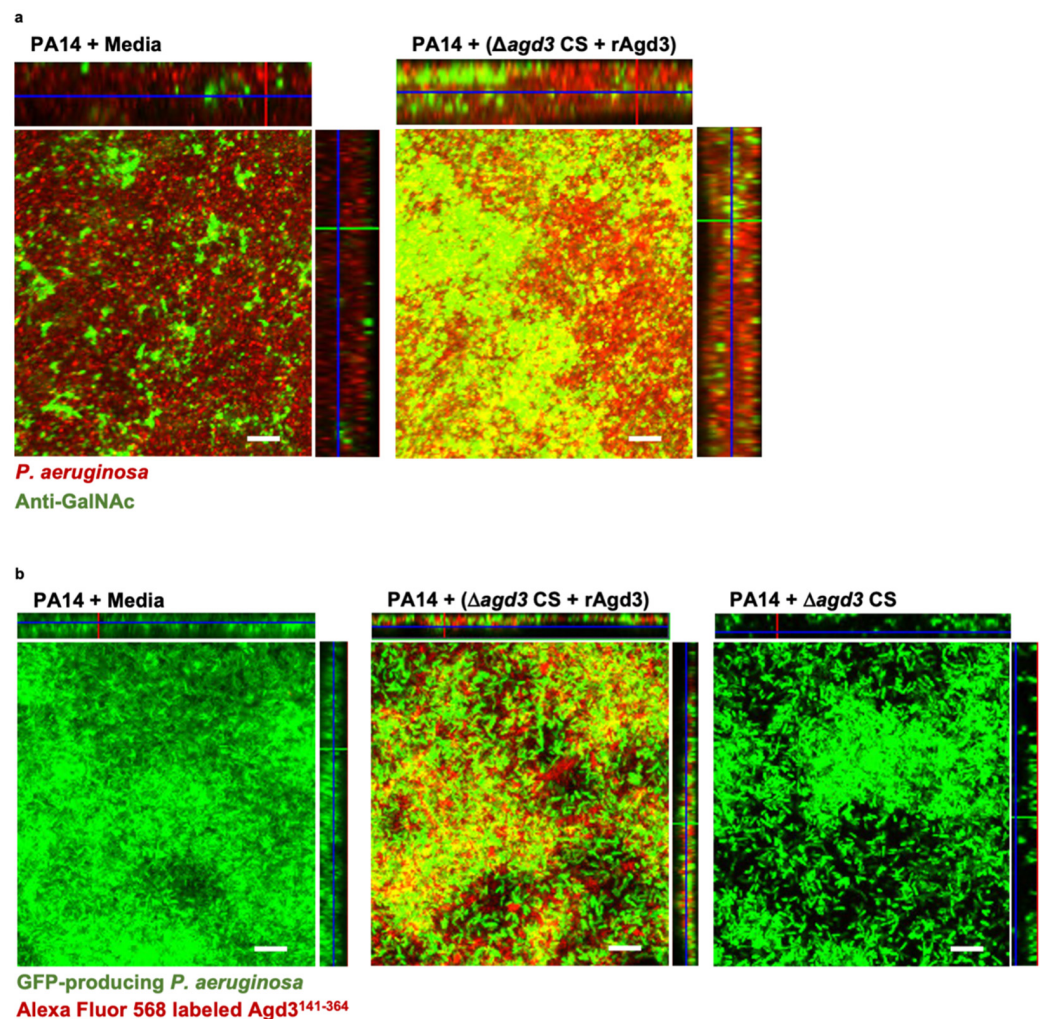


Figure 6. GAG incorporates into *P. aeruginosa* biofilms. (a) Confocal immunofluorescence microscopy maximal intensity projections with orthogonal projections of wild-type *P. aeruginosa* (PA14) biofilms grown in the presence of de-*N*-acetylated GAG from a combination of *N*-acetylated GAG-containing culture supernatants and 165 nM recombinant Agd3 deacetylase ($\Delta agd3$ CS + rAgd3) or media. Exopolysaccharide was detected by staining with anti-*N*-acetyl-D-galactosamine antibody (anti-GalNAc) and an Alexa Fluor-488 conjugated anti-rabbit secondary antibody (green). *P. aeruginosa* was counter stained with DRAQ5 (red). (b) Confocal microscopy maximal intensity projections with orthogonal projections of wild-type green fluorescent protein (GFP)-producing (green) *P. aeruginosa* (PA14) biofilms grown in the presence of de-*N*-acetylated GAG from a combination of $\Delta agd3$ CS and 165 nM rAgd3, $\Delta agd3$ CS alone or in media. Biofilms were imaged with fluorescence microscopy. Exopolysaccharide was detected by staining with Alexa Fluor-568-labeled recombinant carbohydrate binding module Agd3¹⁴¹⁻³⁶⁴ (red). Representative images of 3 independent experiments. Biofilms were imaged at 630 \times (scale bar, 10 μ m).

3.5. GAG-Mediates Resistance to Colistin within *P. aeruginosa* Biofilms

Pel in Pel-dependent *P. aeruginosa* biofilms has been demonstrated to enhance resistance to killing by subinhibitory concentrations of the antibiotic colistin [51]. To determine if GAG incorporation into the biofilm matrix can also enhance the resistance of bacterial biofilms to antimicrobials, the sensitivity of wild-type and GAG-treated *P. aeruginosa* biofilms to colistin was compared. Wild-type and GAG-treated *P. aeruginosa*-adherent biofilms were treated with colistin, and bacterial survival was measured by the quantification of XTT tetrazolium salt metabolism. Consistent with the results of crystal violet experiments (Figure 4a), which suggest that GAG treatment increases the biomass of adher-

ent bacterial biofilms, an increase in bacterial metabolic activity of GAG-treated, adherent *P. aeruginosa* biofilms was observed in comparison to that of wild-type bacterial biofilms (Figure 7). GAG-treated, adherent *P. aeruginosa* biofilms biomass exhibited higher levels of resistance to colistin than wild-type biofilms (decrease of 28% vs. 37% in metabolic activity, respectively) (Figure 7). These data suggest that the secreted GAG that was incorporated into *P. aeruginosa* biofilms could protect against antimicrobial killing at least as well as, if not better than, native bacterial exopolysaccharide.

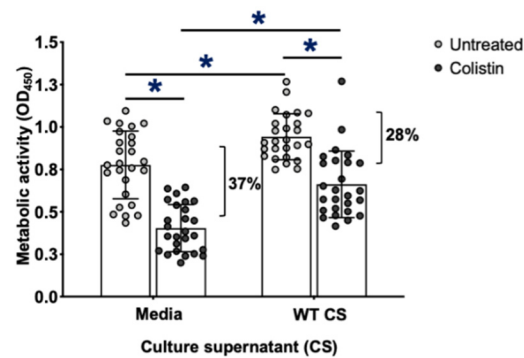


Figure 7. Adherent GAG-treated *P. aeruginosa* biofilms exhibit increased resistance to colistin. Biofilms of wild-type *P. aeruginosa* PA14 were grown in the presence of de-*N*-acetylated GAG-containing culture supernatants from wild-type *A. fumigatus* culture supernatants (WT CS) and then treated with 0.00117 mg/mL of colistin. Viability of *P. aeruginosa* was determined by XTT tetrazolium salt metabolism. Bars represent the means \pm standard deviations of XTT supernatant measured at 450 nm of 5 independent experiments. A significant decrease in absorbance is indicated by * ($p < 0.0005$) between untreated and treated groups and between treated groups and as determined by paired *t* test.

3.6. *P. aeruginosa* Secretes Growth-Inhibitory Products That Counteract the Augmentation of *A. fumigatus*-Adherent Biofilm Formation by Secreted Pel

Given that secreted de-*N*-acetylated GAG can augment the formation of adherent *P. aeruginosa* biofilms, we sought to determine if the opposite was true and if secreted Pel polysaccharide could augment the formation of adherent fungal biofilms. As with GAG, purified Pel is insoluble, and to test this hypothesis, young hyphae (8 h) of wild-type and GAG-deficient Δ *uge3* mutant *A. fumigatus* were co-cultured with culture supernatants from Pel-overproducing Δ *wspF* Δ *psl* P_{BAD} *pel* *P. aeruginosa*. Pel-containing *P. aeruginosa* culture supernatants failed to increase the formation of adherent biofilms by either fungal strain (Figure 8a). Indeed, co-culture with *P. aeruginosa* culture supernatants inhibited wild-type *A. fumigatus* biomass accumulation, consistent with reports of the inhibition of *A. fumigatus* growth and subsequent biofilm formation by a range of small molecules secreted by *P. aeruginosa*. These findings may reflect an inability of Pel to augment adherent *A. fumigatus* biofilm formation, or that the inhibitory effects of small molecules present in *P. aeruginosa* culture supernatants [5–11,17] dominate over any effects that Pel may have on augmenting fungal biofilm formation. Purified Pel is not available; therefore, we were unable to directly test if purified Pel could augment adherent *A. fumigatus* biofilm formation in the absence of bacterial inhibition of fungal growth. *P. aeruginosa* culture supernatants were, therefore, dialyzed to remove inhibitory soluble metabolites prior to co-culture with *A. fumigatus*. The treatment of the GAG-deficient Δ *uge3* *A. fumigatus* mutant with dialyzed culture supernatants from Pel-overproducing *P. aeruginosa* resulted in increased adherent fungal biofilm formation, albeit to a lesser extent than treatment with GAG-containing culture supernatants (Figure 8b). The augmentation of adherent fungal biofilm formation was not observed when *A. fumigatus* was co-cultured with dialyzed *P. aeruginosa* PA14 culture supernatants, suggesting that augmentation of fungal biofilm formation by Pel is dose dependent (Figure 8b). Taken together, these results suggest that while Pel can compensate for the loss of GAG exopolysaccharide and augment adherent biofilm formation by the

GAG-deficient mutant, under standard in vitro conditions, the biofilm inhibitory effects of *P. aeruginosa*-secreted small molecules dominate.

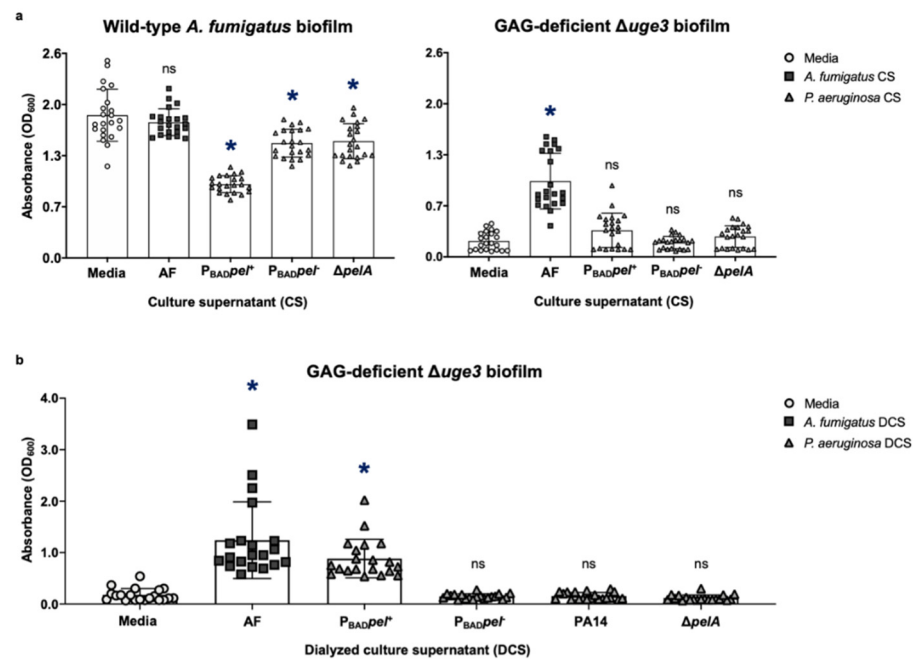


Figure 8. Inhibitory effects on the growth of *A. fumigatus* by secreted products within *P. aeruginosa* culture supernatants that dominate over the augmentation of *A. fumigatus*-adherent biofilm formation by secreted Pel. Adherent biofilm formation by (a) wild-type *A. fumigatus* (AF) (left) and GAG-deficient *A. fumigatus* hyphae ($\Delta uge3$) (right) grown in the presence of culture supernatants (CS) from wild-type *A. fumigatus* (AF), Pel-overexpressing $\Delta wspF\Delta psIP_{BADpel}$ *P. aeruginosa* (P_{BADpel}⁺), Pel-nonexpressing $\Delta wspF\Delta psIP_{BADpel}$ *P. aeruginosa* (P_{BADpel}⁻), or Pel-deficient *P. aeruginosa* ($\Delta pelA$). (b) GAG-deficient *A. fumigatus* hyphae ($\Delta uge3$) grown in the presence of dialyzed culture supernatants (DCS) from wild-type *A. fumigatus* (AF), Pel-overexpressing $\Delta wspF\Delta psIP_{BADpel}$ *P. aeruginosa* (P_{BADpel}⁺), Pel-nonexpressing $\Delta wspF\Delta psIP_{BADpel}$ *P. aeruginosa* (P_{BADpel}⁻), wild-type Pel-dominant *P. aeruginosa* (PA14), or Pel-deficient *P. aeruginosa* ($\Delta pelA$) was quantified with crystal violet staining. Bars represent the means \pm standard deviations of the destain solution measured at 600 nm of at least 3 independent experiments. A significant decrease or increase in absorbance is indicated by * ($p < 0.01$), and no significant difference in absorbance is indicated by ns relative to cultures grown in media alone as determined by one-way ANOVA with Dunnett’s multiple-comparison test.

4. Discussion

Herein, we describe the potential for co-operative biofilm interactions between *A. fumigatus* and *P. aeruginosa*. The contributions of both fungi and bacteria to this interaction were investigated with imaging and biofilm adherence analyses. These studies support previous reports that *A. fumigatus* hyphal GAG mediates the direct binding between these organisms [6] and further elucidates that this interaction is Pel-independent. The dissection of indirect interactions between these species identified the potential for co-operative biofilm interactions mediated by secreted exopolysaccharides. The secreted *A. fumigatus* exopolysaccharide, GAG, was found to physically integrate into bacterial biofilms and could augment resistance to the antibiotic colistin. In contrast, the effects of secreted *P. aeruginosa* products were dominated by the anti-fungal activity of *P. aeruginosa*-secreted products that counteract the Pel-mediated enhancement of *A. fumigatus* biofilms [5,6,8,10,11,16,56–58]. Therefore, this work suggests a potential unidirectional co-operativity in biofilm formation between these organisms.

This study found that hyphal-associated GAG was required for the direct adherence of *P. aeruginosa* to *A. fumigatus*, while the production of bacterial Pel was dispensable for these interactions. A previous study identified the requirement of GAG for the direct interaction of the *P. aeruginosa* PAO1 strain with *A. fumigatus* [59]. However, the *P. aeruginosa* PAO1 strain used in that study predominantly secretes a neutrally charged exopolysaccharide Psl and produces only low levels of Pel [28,36,39,60,61]. Our studies, using Pel-producing, Psl-deficient PA14 and Pel-overexpressing strains, demonstrated that even the overproduction of Pel was insufficient to support the adherence of bacterial cells to *A. fumigatus* hyphae in the absence of GAG. Therefore, direct contact between these organisms is uniquely dependent on GAG.

The resistance of biofilm-forming organisms to antimicrobials is, in part, a consequence of the formation of an exopolysaccharide-containing matrix that impedes the penetration of these molecules [62]. Biofilm exopolysaccharides with a cationic charge can contribute to biofilm resistance to antimicrobials through charge–charge interactions within the matrix [62]. GAG within *A. fumigatus* biofilms mediates resistance to killing by antifungals, likely by repelling cationic molecules or hindering the cellular uptake of large nonpolar molecules [42]. The Pel exopolysaccharide of *P. aeruginosa*, which has a similar chemical structure to GAG, mediates the resistance of *P. aeruginosa* biofilms to the cationic antibiotic colistin, possibly by charge–charge interactions [51]. GAG was found to incorporate into *P. aeruginosa* biofilms, and GAG-augmented bacterial biofilms exhibited an increased resistance to colistin. This observation suggests that the incorporation of a fungal exopolysaccharide did not destabilize the architecture and function of *P. aeruginosa* biofilms. Given the similarities in structure between Pel and GAG, it is plausible that cationic GAG may also mediate resistance to cationic colistin through charge–charge mediated repulsion.

Secreted products from *A. fumigatus* and *P. aeruginosa* have the potential to have pleiotropic effects on the other organism in co-cultures. As of now, studies have largely focused on mutually antagonistic interactions in vitro [5,6,8,9,11,13,17,63]. *A. fumigatus* strains, including the wild-type strain (Af293) used in this study, secrete the mycotoxin gliotoxin that is toxic to *P. aeruginosa* and can be detectable in fungal culture supernatants at as early as 24 h of growth in vitro [64,65]. However, *A. fumigatus* GAG-containing culture supernatants were found to augment the formation of adherent biofilms by the *P. aeruginosa* PA14 strain, suggesting that the ability of GAG to augment bacterial biofilm formation is dominant over any inhibitory effects due to gliotoxin or other toxic secondary metabolites. Similarly, *P. aeruginosa* secrete a plethora of small molecules that have been observed to inhibit *A. fumigatus* growth and biofilm formation [5,6,8,10,11,56]. Consistent with these findings, we found that Pel-containing *P. aeruginosa* cultures' supernatants failed to augment *A. fumigatus*-adherent biofilm formation. The ability of dialyzed culture supernatants from the Pel-overexpressing strain to complement adherent biofilm formation by the GAG-deficient *A. fumigatus* Δ uge3 mutant suggests that, while Pel can act as a surrogate exopolysaccharide for a mutant strain deficient in biofilm adherence under specific conditions, this effect is easily masked by the dominant inhibitory effects of other bacterial secreted factors. Similar evidence for the production of competing compounds by *P. aeruginosa*, which enhance and inhibit fungal growth, was found when the co-operative fungal growth-enhancing effects of bacterial-derived volatile molecules were revealed by physical barrier co-cultures that prevented soluble anti-fungal molecules from contacting *A. fumigatus* in vitro [21,22].

The predominance of studies identifying antagonistic interactions between *P. aeruginosa* with *A. fumigatus* contrasts with the clinical observation that these organisms commonly co-colonize the airways of individuals with chronic lung disease [5,6,9–11,17,56,66]. Our findings provide a potential mechanism whereby these two species that exhibit antagonistic interactions in vitro can conditionally co-operate. A similar co-operative inter-species interaction between *P. aeruginosa* and *C. albicans* has been described at the level of bacterial exopolysaccharide expression. While *P. aeruginosa* directly antagonizes *C. albicans* growth by killing hyphae and indirectly by suppressing filamentation, *C. albicans* is often co-isolated

with *P. aeruginosa* in up to 29% of individuals with cystic fibrosis [67–69]. A metabolite-driven positive feedback loop between bacterial phenazine and *Candida* ethanol production, that was shown to upregulate Pel expression and, consequently, enhance biofilm formation by *P. aeruginosa*, has been postulated to underlie the co-operativity between these two species [70]. Collectively, these studies suggest the possibility that the fungal–bacterial modulation of biofilm adherence or formation may play an important role in the persistence of pulmonary microorganisms in chronic lung disease.

The complex nature of the potential for inhibitory and enhancing interactions between *A. fumigatus* and *P. aeruginosa* suggests that the outcome of the interactions between *A. fumigatus* and *P. aeruginosa* may depend on the microenvironment in which these organisms reside. Further work in animal models of chronic airway co-infection will, therefore, be required to determine the potential significance of the interactions that have been documented in vitro. Currently, however, no model of chronic, non-invasive *Aspergillus/Pseudomonas* co-colonization exists to support these studies. Although chronic airway co-colonization with both organisms has been reported using organisms embedded in agar or other matrix beads [67,69], this model is not suitable to study indirect biofilm interactions, as the use of an exogenous matrix is a potentially major confounder of exopolysaccharide interactions. The findings of our study highlight the need for ex vivo or chronic co-infection models to better dissect *A. fumigatus* and *P. aeruginosa* interactions during chronic airway co-infection.

Our studies demonstrate that a secreted fungal exopolysaccharide can augment adherent bacterial biofilm formation and resistance to antibiotic killing in vitro. Co-operativity may contribute to the worsening of pathogenesis and outcomes in co-colonized individuals. This mechanism of co-operative interactions should be explored in vivo with the development of a relevant and robust co-infection model that can inform treatment outcomes and lead to novel therapeutic strategies.

Supplementary Materials: The following are available online at <https://www.mdpi.com/article/10.3390/jof8040336/s1>, Figure S1: Dose-dependent deacetylation of GAG by recombinant Agd3, Figure S2: Recombinant Agd3 does not exhibit activity on *P. aeruginosa* biofilms, Table S1: A list of fungal and bacterial strains used in this study [71].

Author Contributions: Conceptualization, D.C.S.; methodology, D.C.S., H.O., B.D.S., F.L.M., F.N.G., N.C.B., J.C.V.L. and G.M.; validation, F.L.M.; formal analysis, D.C.S., H.O., F.L.M. and F.N.G.; investigation, H.O., F.N.G. and F.L.M.; writing—original draft preparation, H.O. and D.C.S.; writing—review and editing, H.O., D.C.S., D.N., N.C.B., F.L.M., B.D.S., J.C.V.L. and P.L.H.; funding acquisition, P.L.H. and D.C.S. All authors have read and agreed to the published version of the manuscript.

Funding: This research was funded by Cystic Fibrosis Canada (CFC), grant number 558692, the Canadian Glycomics Network (GlycoNet), grant number AM-15, the United States Army Medical Research and Materiel Command (USAMRMC), grant number W81XWH-15-PRMRP-IIRA, and Canadian Institutes of Health Research (CIHR), grant number 81361. The APC was funded by Cystic Fibrosis Canada (CFC), grant number 558692. N.C.B. was supported in part by Vanier and CGS-M graduate scholarships from the Natural Sciences and Engineering Research Council of Canada (NSERC), Mary H. Beatty, and Dr. James A. and Connie P. Dickson Scholarships from the University of Toronto, Cystic Fibrosis Canada, and The Hospital for Sick Children. P.L.H. was the recipient of a Tier I Canada Research Chair 2006–2020.

Institutional Review Board Statement: Not applicable.

Informed Consent Statement: Not applicable.

Data Availability Statement: Not applicable.

Acknowledgments: This work was performed with the support of the Molecular Imaging platform (Research Institute-McGill University Health Centre) and the Facility for Electron Microscopy Research (Department of Anatomy and Cell Biology, McGill).

Conflicts of Interest: The authors declare no conflict of interest.

References

1. Reece, E.; Segurado, R.; Jackson, A.; McClean, S.; Renwick, J.; Grealley, P. Co-colonisation with *Aspergillus fumigatus* and *Pseudomonas aeruginosa* is associated with poorer health in cystic fibrosis patients: An Irish registry analysis. *BMC Pulm. Med.* **2017**, *17*, 70. [[CrossRef](#)]
2. Valenza, G.; Tappe, D.; Turnwald, D.; Frosch, M.; Konig, C.; Hebestreit, H.; Abele-Horn, M. Prevalence and antimicrobial susceptibility of microorganisms isolated from sputa of patients with cystic fibrosis. *J. Cyst. Fibros.* **2008**, *7*, 123–127. [[CrossRef](#)] [[PubMed](#)]
3. de Vrankrijker, A.M.; van der Ent, C.K.; van Berkhout, F.T.; Stellato, R.K.; Willems, R.J.; Bonten, M.J.; Wolfs, T.F. *Aspergillus fumigatus* colonization in cystic fibrosis: Implications for lung function? *Clin. Microbiol. Infect.* **2011**, *17*, 1381–1386. [[CrossRef](#)] [[PubMed](#)]
4. Amin, R.; Dupuis, A.; Aaron, S.D.; Ratjen, F. The effect of chronic infection with *Aspergillus fumigatus* on lung function and hospitalization in patients with cystic fibrosis. *Chest* **2010**, *137*, 171–176. [[CrossRef](#)]
5. Mowat, E.; Rajendran, R.; Williams, C.; McCulloch, E.; Jones, B.; Lang, S.; Ramage, G. *Pseudomonas aeruginosa* and their small diffusible extracellular molecules inhibit *Aspergillus fumigatus* biofilm formation. *FEMS Microbiol. Lett.* **2010**, *313*, 96–102. [[CrossRef](#)] [[PubMed](#)]
6. Briard, B.; Rasoldier, V.; Bomme, P.; ElAouad, N.; Guerreiro, C.; Chassagne, P.; Muszkieta, L.; Latge, J.P.; Mulard, L.; Beauvais, A. Dirhamnolipids secreted from *Pseudomonas aeruginosa* modify antifungal susceptibility of *Aspergillus fumigatus* by inhibiting beta1,3 glucan synthase activity. *ISME J.* **2017**, *11*, 1578–1591. [[CrossRef](#)] [[PubMed](#)]
7. Davey, M.E.; Caiazza, N.C.; O’Toole, G.A. Rhamnolipid surfactant production affects biofilm architecture in *Pseudomonas aeruginosa* PAO1. *J. Bacteriol.* **2003**, *185*, 1027–1036. [[CrossRef](#)] [[PubMed](#)]
8. Reen, F.J.; Phelan, J.P.; Woods, D.F.; Shanahan, R.; Cano, R.; Clarke, S.; McGlacken, G.P.; O’Gara, F. Harnessing Bacterial Signals for Suppression of Biofilm Formation in the Nosocomial Fungal Pathogen *Aspergillus fumigatus*. *Front. Microbiol.* **2016**, *7*, 2074. [[CrossRef](#)]
9. Sass, G.; Nazik, H.; Penner, J.; Shah, H.; Ansari, S.R.; Clemons, K.V.; Groleau, M.C.; Dietl, A.M.; Visca, P.; Haas, H.; et al. Studies of *Pseudomonas aeruginosa* Mutants Indicate Pyoverdine as the Central Factor in Inhibition of *Aspergillus fumigatus* Biofilm. *J. Bacteriol.* **2018**, *200*, e00345-17. [[CrossRef](#)] [[PubMed](#)]
10. Briard, B.; Mislin, G.L.A.; Latge, J.P.; Beauvais, A. Interactions between *Aspergillus fumigatus* and Pulmonary Bacteria: Current State of the Field, New Data, and Future Perspective. *J. Fungi* **2019**, *5*, 48. [[CrossRef](#)]
11. Briard, B.; Bomme, P.; Lechner, B.E.; Mislin, G.L.; Lair, V.; Prevost, M.C.; Latge, J.P.; Haas, H.; Beauvais, A. *Pseudomonas aeruginosa* manipulates redox and iron homeostasis of its microbiota partner *Aspergillus fumigatus* via phenazines. *Sci. Rep.* **2015**, *5*, 8220. [[CrossRef](#)]
12. Chatterjee, P.; Sass, G.; Swietnicki, W.; Stevens, D.A. Review of Potential *Pseudomonas* Weaponry, Relevant to the *Pseudomonas-Aspergillus* Interplay, for the Mycology Community. *J. Fungi* **2020**, *6*, 81. [[CrossRef](#)]
13. Sass, G.; Nazik, H.; Penner, J.; Shah, H.; Ansari, S.R.; Clemons, K.V.; Groleau, M.C.; Dietl, A.M.; Visca, P.; Haas, H.; et al. *Aspergillus-Pseudomonas* interaction, relevant to competition in airways. *Med. Mycol.* **2019**, *57*, S228–S232. [[CrossRef](#)] [[PubMed](#)]
14. Nazik, H.; Sass, G.; Ansari, S.R.; Ertekin, R.; Haas, H.; Deziel, E.; Stevens, D.A. Novel intermicrobial molecular interaction: *Pseudomonas aeruginosa* Quinolone Signal (QQS) modulates *Aspergillus fumigatus* response to iron. *Microbiology* **2020**, *166*, 44–55. [[CrossRef](#)] [[PubMed](#)]
15. Anand, R.; Moss, R.B.; Sass, G.; Banaei, N.; Clemons, K.V.; Martinez, M.; Stevens, D.A. Small Colony Variants of *Pseudomonas aeruginosa* Display Heterogeneity in Inhibiting *Aspergillus fumigatus* Biofilm. *Mycopathologia* **2018**, *183*, 263–272. [[CrossRef](#)] [[PubMed](#)]
16. Nazik, H.; Sass, G.; Williams, P.; Déziel, E.; Stevens, D.A. Molecular Modifications of the *Pseudomonas* Quinolone Signal in the Intermicrobial Competition with *Aspergillus*. *J. Fungi* **2021**, *7*, 343. [[CrossRef](#)]
17. Penner, J.C.; Ferreira, J.A.G.; Secor, P.R.; Sweere, J.M.; Birukova, M.K.; Joubert, L.M.; Haagsen, J.A.J.; Garcia, O.; Malkovskiy, A.V.; Kaber, G.; et al. Pf4 bacteriophage produced by *Pseudomonas aeruginosa* inhibits *Aspergillus fumigatus* metabolism via iron sequestration. *Microbiology* **2016**, *162*, 1583–1594. [[CrossRef](#)] [[PubMed](#)]
18. Nazik, H.; Sass, G.; Deziel, E.; Stevens, D.A. *Aspergillus* Is Inhibited by *Pseudomonas aeruginosa* Volatiles. *J. Fungi* **2020**, *6*, 118. [[CrossRef](#)]
19. Hunter, R.C.; Asfour, F.; Dingemans, J.; Osuna, B.L.; Samad, T.; Malfroot, A.; Cornelis, P.; Newman, D.K. Ferrous iron is a significant component of bioavailable iron in cystic fibrosis airways. *mBio* **2013**, *4*, e00557-13. [[CrossRef](#)]
20. Wang, Y.; Newman, D.K. Redox reactions of phenazine antibiotics with ferric (hydr)oxides and molecular oxygen. *Environ. Sci. Technol.* **2008**, *42*, 2380–2386. [[CrossRef](#)]
21. Scott, J.; Sueiro-Olivares, M.; Ahmed, W.; Heddergott, C.; Zhao, C.; Thomas, R.; Bromley, M.; Latge, J.P.; Krappmann, S.; Fowler, S.; et al. *Pseudomonas aeruginosa*-Derived Volatile Sulfur Compounds Promote Distal *Aspergillus fumigatus* Growth and a Synergistic Pathogen-Pathogen Interaction That Increases Pathogenicity in Co-infection. *Front. Microbiol.* **2019**, *10*, 2311. [[CrossRef](#)] [[PubMed](#)]
22. Briard, B.; Heddergott, C.; Latge, J.P. Volatile Compounds Emitted by *Pseudomonas aeruginosa* Stimulate Growth of the Fungal Pathogen *Aspergillus fumigatus*. *mBio* **2016**, *7*, e00219-16. [[CrossRef](#)]

23. Gravelat, F.N.; Beauvais, A.; Liu, H.; Lee, M.J.; Snarr, B.D.; Chen, D.; Xu, W.; Kravtsov, I.; Hoareau, C.M.; Vanier, G.; et al. *Aspergillus galactosaminogalactan mediates adherence to host constituents and conceals hyphal beta-glucan from the immune system. PLoS Pathog.* **2013**, *9*, e1003575. [[CrossRef](#)]
24. Lee, M.J.; Geller, A.M.; Bamford, N.C.; Liu, H.; Gravelat, F.N.; Snarr, B.D.; Le Mauff, F.; Chabot, J.; Ralph, B.; Ostapska, H.; et al. Deacetylation of Fungal Exopolysaccharide Mediates Adhesion and Biofilm Formation. *mBio* **2016**, *7*, e00252-16. [[CrossRef](#)] [[PubMed](#)]
25. Colvin, K.M.; Alnabseya, N.; Baker, P.; Whitney, J.C.; Howell, P.L.; Parsek, M.R. PelA deacetylase activity is required for Pel polysaccharide synthesis in *Pseudomonas aeruginosa*. *J. Bacteriol.* **2013**, *195*, 2329–2339. [[CrossRef](#)] [[PubMed](#)]
26. Colvin, K.M.; Gordon, V.D.; Murakami, K.; Borlee, B.R.; Wozniak, D.J.; Wong, G.C.; Parsek, M.R. The pel polysaccharide can serve a structural and protective role in the biofilm matrix of *Pseudomonas aeruginosa*. *PLoS Pathog.* **2011**, *7*, e1001264. [[CrossRef](#)]
27. Fontaine, T.; Delangle, A.; Simenel, C.; Coddeville, B.; van Vliet, S.J.; van Kooyk, Y.; Bozza, S.; Moretti, S.; Schwarz, F.; Trichot, C.; et al. Galactosaminogalactan, a new immunosuppressive polysaccharide of *Aspergillus fumigatus*. *PLoS Pathog.* **2011**, *7*, e1002372. [[CrossRef](#)]
28. Jennings, L.K.; Storek, K.M.; Ledvina, H.E.; Coulon, C.; Marmont, L.S.; Sadovskaya, I.; Secor, P.R.; Tseng, B.S.; Scian, M.; Filloux, A.; et al. Pel is a cationic exopolysaccharide that cross-links extracellular DNA in the *Pseudomonas aeruginosa* biofilm matrix. *Proc. Natl. Acad. Sci. USA* **2015**, *112*, 11353–11358. [[CrossRef](#)] [[PubMed](#)]
29. Jennings, L.K.; Dreifus, J.E.; Reichhardt, C.; Storek, K.M.; Secor, P.R.; Wozniak, D.J.; Hisert, K.B.; Parsek, M.R. *Pseudomonas aeruginosa* aggregates in cystic fibrosis sputum produce exopolysaccharides that likely impede current therapies. *Cell Rep.* **2021**, *34*, 108782. [[CrossRef](#)] [[PubMed](#)]
30. Sheppard, D.C.; Howell, P.L. Biofilm Exopolysaccharides of Pathogenic Fungi: Lessons from Bacteria. *J. Biol. Chem.* **2016**, *291*, 12529–12537. [[CrossRef](#)] [[PubMed](#)]
31. Franklin, M.J.; Nivens, D.E.; Weadge, J.T.; Howell, P.L. Biosynthesis of the *Pseudomonas aeruginosa* Extracellular Polysaccharides, Alginate, Pel, and Psl. *Front. Microbiol.* **2011**, *2*, 167. [[CrossRef](#)] [[PubMed](#)]
32. Bamford, N.C.; Le Mauff, F.; Van Loon, J.C.; Ostapska, H.; Snarr, B.D.; Zhang, Y.; Kitova, E.N.; Klassen, J.S.; Codée, J.D.C.; Sheppard, D.C.; et al. Structural and biochemical characterization of the exopolysaccharide deacetylase Agd3 required for *Aspergillus fumigatus* biofilm formation. *Nat. Commun.* **2020**, *11*, 2450. [[CrossRef](#)] [[PubMed](#)]
33. Whitfield, G.B.; Marmont, L.S.; Ostaszewski, A.; Rich, J.D.; Whitney, J.C.; Parsek, M.R.; Harrison, J.J.; Howell, P.L. Pel polysaccharide biosynthesis requires an inner membrane complex comprised of PelD, PelE, PelF and PelG. *J. Bacteriol.* **2020**, *202*, e00684-19. [[CrossRef](#)] [[PubMed](#)]
34. Marmont, L.S.; Rich, J.D.; Whitney, J.C.; Whitfield, G.B.; Almblad, H.; Robinson, H.; Parsek, M.R.; Harrison, J.J.; Howell, P.L. Oligomeric lipoprotein PelC guides Pel polysaccharide export across the outer membrane of *Pseudomonas aeruginosa*. *Proc. Natl. Acad. Sci. USA* **2017**, *114*, 2892–2897. [[CrossRef](#)]
35. Lee, D.G.; Urbach, J.M.; Wu, G.; Liberati, N.T.; Feinbaum, R.L.; Miyata, S.; Diggins, L.T.; He, J.; Saucier, M.; Déziel, E.; et al. Genomic analysis reveals that *Pseudomonas aeruginosa* virulence is combinatorial. *Genome Biol.* **2006**, *7*, R90. [[CrossRef](#)]
36. Colvin, K.M.; Irie, Y.; Tart, C.S.; Urbano, R.; Whitney, J.C.; Ryder, C.; Howell, P.L.; Wozniak, D.J.; Parsek, M.R. The Pel and Psl polysaccharides provide *Pseudomonas aeruginosa* structural redundancy within the biofilm matrix. *Environ. Microbiol.* **2012**, *14*, 1913–1928. [[CrossRef](#)]
37. Friedman, L.; Kolter, R. Genes involved in matrix formation in *Pseudomonas aeruginosa* PA14 biofilms. *Mol. Microbiol.* **2004**, *51*, 675–690. [[CrossRef](#)]
38. Stover, C.K.; Pham, X.Q.; Erwin, A.L.; Mizoguchi, S.D.; Warren, P.; Hickey, M.J.; Brinkman, F.S.L.; Hufnagle, W.O.; Kowalik, D.J.; Lagrou, M.; et al. Complete genome sequence of *Pseudomonas aeruginosa* PAO1, an opportunistic pathogen. *Nature* **2000**, *406*, 959–964. [[CrossRef](#)]
39. Yang, L.; Hu, Y.; Liu, Y.; Zhang, J.; Ulstrup, J.; Molin, S. Distinct roles of extracellular polymeric substances in *Pseudomonas aeruginosa* biofilm development. *Environ. Microbiol.* **2011**, *13*, 1705–1717. [[CrossRef](#)]
40. Jackson, K.D.; Starkey, M.; Kremer, S.; Parsek, M.R.; Wozniak, D.J. Identification of psl, a locus encoding a potential exopolysaccharide that is essential for *Pseudomonas aeruginosa* PAO1 biofilm formation. *J. Bacteriol.* **2004**, *186*, 4466–4475. [[CrossRef](#)]
41. Choi, K.H.; Kumar, A.; Schweizer, H.P. A 10-min method for preparation of highly electrocompetent *Pseudomonas aeruginosa* cells: Application for DNA fragment transfer between chromosomes and plasmid transformation. *J. Microbiol. Methods* **2006**, *64*, 391–397. [[CrossRef](#)] [[PubMed](#)]
42. Snarr, B.D.; Baker, P.; Bamford, N.C.; Sato, Y.; Liu, H.; Lehoux, M.; Gravelat, F.N.; Ostapska, H.; Baistrocchi, S.R.; Cerone, R.P.; et al. Microbial glycoside hydrolases as antibiofilm agents with cross-kingdom activity. *Proc. Natl. Acad. Sci. USA* **2017**, *114*, 7124–7129. [[CrossRef](#)] [[PubMed](#)]
43. Gravelat, F.N.; Askew, D.S.; Sheppard, D.C. Targeted gene deletion in *Aspergillus fumigatus* using the hygromycin-resistance split-marker approach. *Methods Mol. Biol.* **2012**, *845*, 119–130. [[CrossRef](#)] [[PubMed](#)]
44. Ejzykiewicz, D.E.; Cunha, M.M.; Rozental, S.; Solis, N.V.; Gravelat, F.N.; Sheppard, D.C.; Filler, S.G. The *Aspergillus fumigatus* transcription factor Ace2 governs pigment production, conidiation and virulence. *Mol. Microbiol.* **2009**, *72*, 155–169. [[CrossRef](#)] [[PubMed](#)]
45. Gravelat, F.N.; Ejzykiewicz, D.E.; Chiang, L.Y.; Chabot, J.C.; Urb, M.; Macdonald, K.D.; al-Bader, N.; Filler, S.G.; Sheppard, D.C. *Aspergillus fumigatus* MedA governs adherence, host cell interactions and virulence. *Cell. Microbiol.* **2010**, *12*, 473–488. [[CrossRef](#)]

46. Urb, M.; Snarr, B.D.; Wojewodka, G.; Lehoux, M.; Lee, M.J.; Ralph, B.; Divangahi, M.; King, I.L.; McGovern, T.K.; Martin, J.G.; et al. Evolution of the Immune Response to Chronic Airway Colonization with *Aspergillus fumigatus* Hyphae. *Infect. Immun.* **2015**, *83*, 3590–3600. [[CrossRef](#)]
47. Sheppard, D.C.; Marr, K.A.; Fredricks, D.N.; Chiang, L.Y.; Doedt, T.; Filler, S.G. Comparison of three methodologies for the determination of pulmonary fungal burden in experimental murine aspergillosis. *Clin. Microbiol. Infect.* **2006**, *12*, 376–380. [[CrossRef](#)]
48. Liu, H.; Gravelat, F.N.; Chiang, L.Y.; Chen, D.; Vanier, G.; Ejzykowicz, D.E.; Ibrahim, A.S.; Nierman, W.C.; Sheppard, D.C.; Filler, S.G. *Aspergillus fumigatus* AcuM regulates both iron acquisition and gluconeogenesis. *Mol. Microbiol.* **2010**, *78*, 1038–1054. [[CrossRef](#)]
49. Al-Bader, N.; Vanier, G.; Liu, H.; Gravelat, F.N.; Urb, M.; Hoareau, C.M.; Campoli, P.; Chabot, J.; Filler, S.G.; Sheppard, D.C. Role of trehalose biosynthesis in *Aspergillus fumigatus* development, stress response, and virulence. *Infect. Immun.* **2010**, *78*, 3007–3018. [[CrossRef](#)]
50. Beaudoin, T.; Kennedy, S.; Yau, Y.; Waters, V. Visualizing the Effects of Sputum on Biofilm Development Using a Chambered Coverglass Model. *J. Vis. Exp.* **2016**, *118*, e54819. [[CrossRef](#)]
51. Baker, P.; Hill, P.J.; Snarr, B.D.; Alnabelseya, N.; Pestrak, M.J.; Lee, M.J.; Jennings, L.K.; Tam, J.; Melnyk, R.A.; Parsek, M.R.; et al. Exopolysaccharide biosynthetic glycoside hydrolases can be utilized to disrupt and prevent *Pseudomonas aeruginosa* biofilms. *Sci. Adv.* **2016**, *2*, e1501632. [[CrossRef](#)] [[PubMed](#)]
52. Pierce, C.G.; Uppuluri, P.; Tristan, A.R.; Wormley, F.L., Jr.; Mowat, E.; Ramage, G.; Lopez-Ribot, J.L. A simple and reproducible 96-well plate-based method for the formation of fungal biofilms and its application to antifungal susceptibility testing. *Nat. Protoc.* **2008**, *3*, 1494–1500. [[CrossRef](#)] [[PubMed](#)]
53. Ostapska, H.; Raju, D.; Lehoux, M.; Lacdao, I.; Gilbert, S.; Sivarajah, P.; Bamford, N.C.; Baker, P.; Nguyen, T.T.M.; Zacharias, C.A.; et al. Preclinical Evaluation of Recombinant Microbial Glycoside Hydrolases in the Prevention of Experimental Invasive Aspergillosis. *mBio* **2021**, *12*, e0244621. [[CrossRef](#)] [[PubMed](#)]
54. Ralph, B.A.; Lehoux, M.; Ostapska, H.; Snarr, B.D.; Caffrey-Carr, A.K.; Fraser, R.; Saleh, M.; Obar, J.J.; Qureshi, S.T.; Sheppard, D.C. The IL-1 Receptor Is Required to Maintain Neutrophil Viability and Function During *Aspergillus fumigatus* Airway Infection. *Front. Immunol.* **2021**, *12*, 675294. [[CrossRef](#)] [[PubMed](#)]
55. Ejzykowicz, D.E.; Solis, N.V.; Gravelat, F.N.; Chabot, J.; Li, X.; Sheppard, D.C.; Filler, S.G. Role of *Aspergillus fumigatus* DvrA in host cell interactions and virulence. *Eukaryot. Cell* **2010**, *9*, 1432–1440. [[CrossRef](#)] [[PubMed](#)]
56. Kerr, J.R.; Taylor, G.W.; Rutman, A.; Hoiby, N.; Cole, P.J.; Wilson, R. *Pseudomonas aeruginosa* pyocyanin and 1-hydroxyphenazine inhibit fungal growth. *J. Clin. Pathol.* **1999**, *52*, 385–387. [[CrossRef](#)] [[PubMed](#)]
57. Shirazi, F.; Ferreira, J.A.; Stevens, D.A.; Clemons, K.V.; Kontoyiannis, D.P. Biofilm Filtrates of *Pseudomonas aeruginosa* Strains Isolated from Cystic Fibrosis Patients Inhibit Preformed *Aspergillus fumigatus* Biofilms via Apoptosis. *PLoS ONE* **2016**, *11*, e0150155. [[CrossRef](#)]
58. Ferreira, J.A.; Penner, J.C.; Moss, R.B.; Haagensen, J.A.; Clemons, K.V.; Spormann, A.M.; Nazik, H.; Cohen, K.; Banaei, N.; Carolino, E.; et al. Inhibition of *Aspergillus fumigatus* and Its Biofilm by *Pseudomonas aeruginosa* Is Dependent on the Source, Phenotype and Growth Conditions of the Bacterium. *PLoS ONE* **2015**, *10*, e0134692. [[CrossRef](#)]
59. Lee, H.; Krebs, H.I.; Hogan, N. Multivariable dynamic ankle mechanical impedance with active muscles. *IEEE Trans. Neural Syst. Rehabil. Eng.* **2014**, *22*, 971–981. [[CrossRef](#)]
60. Byrd, M.S.; Sadovskaya, I.; Vinogradov, E.; Lu, H.; Sprinkle, A.B.; Richardson, S.H.; Ma, L.; Ralston, B.; Parsek, M.R.; Anderson, E.M.; et al. Genetic and biochemical analyses of the *Pseudomonas aeruginosa* Psl exopolysaccharide reveal overlapping roles for polysaccharide synthesis enzymes in Psl and LPS production. *Mol. Microbiol.* **2009**, *73*, 622–638. [[CrossRef](#)]
61. Ghafoor, A.; Hay, I.D.; Rehm, B.H. Role of exopolysaccharides in *Pseudomonas aeruginosa* biofilm formation and architecture. *Appl. Environ. Microbiol.* **2011**, *77*, 5238–5246. [[CrossRef](#)] [[PubMed](#)]
62. Ostapska, H.; Howell, P.L.; Sheppard, D.C. Deacetylated microbial biofilm exopolysaccharides: It pays to be positive. *PLoS Pathog.* **2018**, *14*, e1007411. [[CrossRef](#)]
63. Reece, E.; Doyle, S.; Greally, P.; Renwick, J.; McClean, S. *Aspergillus fumigatus* Inhibits *Pseudomonas aeruginosa* in Co-culture: Implications of a Mutually Antagonistic Relationship on Virulence and Inflammation in the CF Airway. *Front. Microbiol.* **2018**, *9*, 1205. [[CrossRef](#)]
64. Reeves, E.P.; Messina, C.G.; Doyle, S.; Kavanagh, K. Correlation between gliotoxin production and virulence of *Aspergillus fumigatus* in *Galleria mellonella*. *Mycopathologia* **2004**, *158*, 73–79. [[CrossRef](#)] [[PubMed](#)]
65. Lewis, R.E.; Wiederhold, N.P.; Lionakis, M.S.; Prince, R.A.; Kontoyiannis, D.P. Frequency and species distribution of gliotoxin-producing *Aspergillus* isolates recovered from patients at a tertiary-care cancer center. *J. Clin. Microbiol.* **2005**, *43*, 6120–6122. [[CrossRef](#)] [[PubMed](#)]
66. Bakare, N.; Rickerts, V.; Bargon, J.; Just-Nubling, G. Prevalence of *Aspergillus fumigatus* and other fungal species in the sputum of adult patients with cystic fibrosis. *Mycoses* **2003**, *46*, 19–23. [[CrossRef](#)]
67. Hogan, D.A.; Kolter, R. *Pseudomonas-Candida* interactions: An ecological role for virulence factors. *Science* **2002**, *296*, 2229–2232. [[CrossRef](#)] [[PubMed](#)]
68. Hogan, D.A.; Vik, A.; Kolter, R. A *Pseudomonas aeruginosa* quorum-sensing molecule influences *Candida albicans* morphology. *Mol. Microbiol.* **2004**, *54*, 1212–1223. [[CrossRef](#)] [[PubMed](#)]

69. Haiko, J.; Saeedi, B.; Bagger, G.; Karpati, F.; Özenci, V. Coexistence of *Candida* species and bacteria in patients with cystic fibrosis. *Eur. J. Clin. Microbiol. Infect. Dis.* **2019**, *38*, 1071–1077. [[CrossRef](#)] [[PubMed](#)]
70. Chen, A.I.; Dolben, E.F.; Okegbe, C.; Harty, C.E.; Golub, Y.; Thao, S.; Ha, D.G.; Willger, S.D.; O'Toole, G.A.; Harwood, C.S.; et al. *Candida albicans* ethanol stimulates *Pseudomonas aeruginosa* WspR-controlled biofilm formation as part of a cyclic relationship involving phenazines. *PLoS Pathog.* **2014**, *10*, e1004480. [[CrossRef](#)]
71. Campoli, P.; Al Abdallah, Q.; Robitaille, R.; Solis, N.V.; Fielhaber, J.A.; Kristof, A.S.; Laverdiere, M.; Filler, S.G.; Sheppard, D.C. Concentration of antifungal agents within host cell membranes: A new paradigm governing the efficacy of prophylaxis. *Antimicrob. Agents Chemother.* **2011**, *55*, 5732–5739. [[CrossRef](#)] [[PubMed](#)]